SCIENCE CHINA
Physics, Mechanics & Astronomy

• Article •
Progress of Projects Supported by NSFC

December 2012 Vol.55 No.12: 2237–2243
doi: 10.1007/s11433-012-4949-5

Competition between attraction and diffusion in nanoscale non-equilibrium aggregation

WANG BoYang, DENG Li & WANG YanTing*

State Key Laboratory of Theoretical Physics, Institute of Theoretical Physics, Chinese Academy of Sciences, Beijing 100190, China

Received October 31, 2012; accepted November 7, 2012; published online November 21, 2012

The competition between attraction and diffusion determines the kinetics of non-equilibrium aggregation process. The formation of silver nanoclusters through non-equilibrium aggregation of silver atoms in solution was simulated by molecular dynamics as a model system to study the influence of the competition between attraction and diffusion on the aggregation process by varying concentration and temperature. It has been found that the aggregation time decreases monotonically with increasing concentration of silver atoms because of increasing attraction, while initially decreasing and then increasing with increasing temperature because of the competition between accelerated attractive motion and increasing diffusive motion of silver atoms. A mean field approximation was employed to develop a phenomenological model describing the mechanism of temperature dependence of aggregation time.

diffusion, interaction, nanoparticles, molecular dynamics simulation

PACS number(s): 34.10.+x, 34.20.-b, 82.20.-w, 82.20.Wt, 82.20.Fd

Citation: Wang B Y, Deng L, Wang Y T. Competition between attraction and diffusion in nanoscale non-equilibrium aggregation. Sci China-Phys Mech Astron, 2012, 55: 2237–2243, doi: 10.1007/s11433-012-4949-5

1 Introduction

Aggregation [1–3], nucleation [4], and self-assembly [5–7] processes are closely related non-equilibrium processes in physical and chemical systems, similar in that they all involve association of atoms, clusters, or molecules. Two major types of movements generally compete in these processes: association of particles because of attractive interactions between monomers, and the random walk of particles because of the diffusive motion at a finite temperature. A number of theoretical studies have been focused on certain processes, such as gas phase nucleation processes [8–10], diffusion limited aggregation (DLA) of hard spheres [1–3], and colloidal self-assembly processes [11,12]. However, there are still no general theoretical frameworks which describe how the competition between attraction and diffusion can determine the kinetics of those processes.

Classical nucleation theory [4,8,9,13–16] assumes that the system evolves near equilibrium, so the size distribution of the formed particles approximately obeys the Boltzmann distribution. Under this assumption, the rate of the nucleation process is proportional to $\exp(-\Delta G / RT)$, where R is the gas constant, T is the temperature of the system, ΔG is the free energy change of the process. The kinetics of aggregation can also be described by the master equation for reversible aggregation processes [14,17–19]. The simplest version [14] of the master equation is given as:

$$\frac{\mathrm{d}P(\boldsymbol{N},t)}{\mathrm{d}t} = \frac{1}{2V}\sum_{i,j} k_{ij}[(N_i+1)(N_j+1+\delta_{ij}) P(\boldsymbol{N}_{ij}^{+},t) - N_i(N_j-\delta_{ij})P(\boldsymbol{N},t)],$$

*Corresponding author (email: wangyt@itp.ac.cn)

$$+\frac{1}{2V}\sum_{n=2}^{\infty}\left[(N_n+1)\sum_{i=1}^{n-1}f_{i(n-i)}P(\boldsymbol{N}_{i(n-i)}^{-},t)-N_n\sum_{i=1}^{n-1}f_{i(n-i)}P(\boldsymbol{N},t)\right], \quad (1)$$

where $P(\boldsymbol{N}, t)$ is the probability of finding the system in the state $\boldsymbol{N}=(N_1,N_2, ..., N_n)$ at time t, N_i is the number of clusters with size i, k_{ij} is the aggregation kernel that corresponds to the aggregation rate constant, and f_{ij} is the fragmentation kernel that corresponds to the fragmentation rate constant. $\boldsymbol{N}_{ij}^{+}$ are those states which by following a single aggregation event, may produce the state $\boldsymbol{N}$, and $\boldsymbol{N}_{ij}^{-}$ are the states which may produce $\boldsymbol{N}$ by breaking a cluster into two parts. Neither of these two theories, however, is suitable for describing the competition between attraction and diffusion in non-equilibrium aggregation processes.

For a general aggregation process in which monomers join each other and form larger and fewer particles as time goes by, the size distribution of the formed particles as a function of time can be described by the kinetic equation as given by Babu et al. [2,20–22],

$$\frac{\mathrm{d}N_m}{\mathrm{d}t}=\frac{1}{2}\sum_{i+j=m}K_{ij}N_iN_j-\sum_j K_{mj}N_mN_j. \quad (2)$$

Here, m is the number of basic aggregation units in a formed particle, N_m is the number of particles with m basic aggregation units, K_{ij} is the cohesion rate at which a cluster with size i collides with a cluster with size j. In the limiting case of DLA [1,2], when the particles do not interact with each other and only do pure random-walk diffusion before they come close enough and stick together, the cohesion rate is $K_{ij}=4\pi(R_{\mathrm{col},i}+R_{\mathrm{col},j})(D_i+D_j)$, with R_{col} the collision radius of particles, and D the diffusion coefficient of clusters. For more general cases, attraction is also present in addition to diffusion, and DLA is no longer a good theoretical description for those cases, not only because attraction accelerates movements of particles towards each other, but also because diffusion kinetics can be altered by attraction. The attraction and diffusion compete [14,15], and each of them may dominate at different temperatures, concentrations, and attraction strengths. However, no general solutions for eq. (2) are currently available for the cases beyond DLA.

A recent study[1)] has discovered that, in a $AgNO_3$ solution, when Ag atoms are reduced by Cu atoms, the Ag atoms first undergo a fast process to aggregate locally and form Ag nanoclusters, before the nanoclusters undergo a slower process to self-assemble into dendritic intermediate structures. Both steps are non-equilibrium aggregation self-assembly processes involving the competition between attractive and diffusive motions. The kinetics of the aggregation processes with respect to concentration and temperature are important for understanding the formation of nanoclusters and dendritic structures.

In this work, we use molecular dynamics (MD) simulations to study the kinetics of non-equilibrium aggregation of silver atoms forming silver nanoclusters in an aqueous solution. The motivation of this work is not only providing useful information for understanding specifically the initial step of silver nanocluster formation in the whole self-assembly process of silver dendrites, but also investigating more generally the competitive relationship between attraction and diffusion in non-equilibrium aggregation processes by using the silver atom system as a model system. This system is relatively simple and can serve as a good model which grasps the essence of general aggregation processes, but is still complex enough to correspond to a real system. Our simulation results indicate that the aggregation time of individual Ag atoms decreases monotonically with concentration, but first decreases and then increases with temperature. This qualitative conclusion can be considered quite general and independent of the details of the model and methods we have used for our simulations of silver atoms. A phenomenological model for aggregation time with respect to temperature was developed based on a physical argument of the temperature dependence of the competition between attraction and diffusion. Although this empirical model has been constructed from one special case, we believe its physical interpretation is considerably more general in depicting the competitive relationship between attraction and diffusion in aggregation, nucleation, self-assembly, as well as other related physical and chemical processes.

2 Methods

Our MD simulations were performed by using LAMMPS software package [23] and the interactions between silver atoms were modeled by the Embedded Atom Model [24], a widely used general force field for metals. Periodic boundary conditions were applied in all three dimensions of a cubic simulation box. Initially, 1000 silver atoms were uniformly distributed in a cubic simulation box (Figure 1(a)). We set the atoms in a 3D lattice to mimic the condition when the Ag atoms are uniformly dispersed in the solution before the aggregation process begins. It is also possible to arrange the original positions of silver atoms randomly in the simulation box. Our simulation results (data not shown) demonstrate that the kinetics of aggregation is insensitive to the structure of the initial configuration.

At the beginning of the MD simulations, random velocities are assigned to silver atoms in such a way that the system has an initial temperature T. The system then evolves with time according to the stochastic Langevin equations of motion [25] to simulate the silver atoms in an implicit

1) Zhou Q, Wang B, Wang P J, et al. Nanoparticle-based crystal growth via self-assembly. Submitted

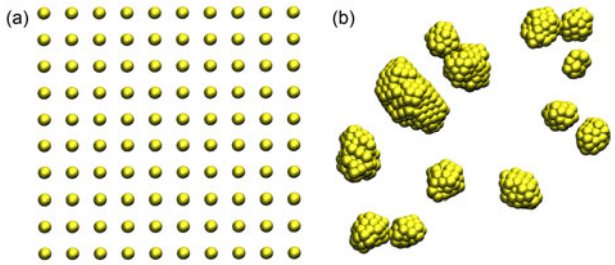

Figure 1 (Color online) Initial (a) and final (b) configurations of a system with 1000 silver atoms simulated for 40 ns at T= 300 K. The periodic cubic simulation box has a side length of a = 10 nm (corresponding to a concentration of 1.66 mol/L).

solvent:

$$m_i \frac{\mathrm{d}^2 \boldsymbol{r}_i(t)}{\mathrm{d}t^2} = \boldsymbol{F}_i + \boldsymbol{R}_i - m_i \gamma_i \frac{\mathrm{d}\boldsymbol{r}_i(t)}{\mathrm{d}t}. \quad (3)$$

Here, $\boldsymbol{r}_i(t)$ is the position of atom i at time t, m_i is its mass, and $\boldsymbol{F}_i$ is the total force on atom i because of the interactions from other atoms. In eq. (3), two terms are added to the Newton's equations of motion: a stochastic force $\boldsymbol{R}_i$, and a frictional force proportional to a damping coefficient γ_i, to mimic the Brownian motion of silver atoms in an aqueous solution. These two terms damp the particle velocities and couple the system with a virtual reservoir with a constant temperature T. $\boldsymbol{R}_i$ obeys a Gaussian process whose correlation time is infinitely short (i.e., the process is Markovian). According to the fluctuation-dissipation theorem [25], if the system is in thermal equilibrium with the reservoir at temperature T, then the power spectrum of $\boldsymbol{R}_i$ is a constant,

$$2\pi G(\omega) = \int_{-\infty}^{\infty} \left\langle \boldsymbol{R}_i(t_0 + t)\boldsymbol{R}_i(t_0) \right\rangle \mathrm{e}^{-\mathrm{i}\omega t} \mathrm{d}t = 2m_i k_\mathrm{B} T \gamma_i, \quad (4)$$

where k_B is the Boltzmann constant, T is the Langevin temperature, and the power spectrum $G(\omega)$ is the Fourier transform of the auto-correlation function $R_i(t)$.

We model the implicit water solvent [26] by setting the damping coefficient $\gamma = 6\pi\eta r / m$, where η, r, m are the viscosity of water at T, the radius, and mass of silver atoms, respectively. The water viscosity η is fitted and extrapolated to higher temperatures by $\eta = \eta_0 \exp(-bT)$, where η_0, b are constants, and for water, b=0.0174 K^{-1}, and η_0=0.164 Pa·s [27,28]. Here we take m=107.87 au, and r = 1.45 Å, because the closest distance between two silver atoms in the fcc silver crystal is approximately 2.89 Å, as calculated from the lattice constant of 4.09 Å. For example, at T = 300 K, η = 8.90×10^{-4} Pa·s, and thus $\gamma \approx 4.78$ ps^{-1}.

3 Results and discussion

Stochastic Langevin dynamics simulations were performed for the aggregation of 1000 silver atoms at different temperatures from 300 K to 900 K with an interval of 100 K. At each temperature, the simulations were conducted at different concentrations of c=1.66, 0.106, 0.0133, 0.00393, and 0.00166 mol/L, corresponding to the side lengths of the simulation box a=10, 25, 50, 75, and 100 nm, respectively. The total number of particles $N(t)$ during the aggregation process was approximately counted by regarding two silver atoms as belonging to the same cluster when their distance is less than 4.0 Å.

Figure 1(b) shows the final configuration of the system at T=300 K, and c=1.66 mol/L, after 40 ns of aggregation. Because of the strong attraction between Ag atoms, they quickly form small clusters locally. Although the atoms initially stick together randomly to form arbitrary structures, our simulation results indicate that it takes less than 10 ps for the small clusters to adjust to the optimized structures. For example, a 3-atom cluster finally becomes a triangle, and a 4-atom cluster finally assumes a tetrahedral shape. As time goes by, these small clusters further aggregate and form larger silver nanoparticles, as those shown in Figure 1(b). Because the attractive forces between silver atoms are relatively strong, the aggregation of silver atoms and nanoparticles is a non-equilibrium irreversible process.

To characterize the kinetics of this non-equilibrium aggregation process, we calculate the total number of particles $N(t)$, including both individual silver atoms and nanoparticles in the system, as a function of time. In Figure 2, we plot $N(t)$ at different temperatures, with a concentration of c= 0.0133 mol/L (corresponding to a= 50 nm). We can see that, at each temperature, $N(t)$ decreases somewhat as an exponential decay function. At temperatures lower than 600 K, the aggregation time is shorter when the temperature increases, because attraction dominates and the particles move faster towards each other at higher temperatures because of increased velocities. The aggregation time becomes longer at a higher temperature when T>600 K, because diffusion dominates and the particles statistically move along a longer random-walk trajectory before they bump into each other and aggregate. After about 60 ns, the aggregation at

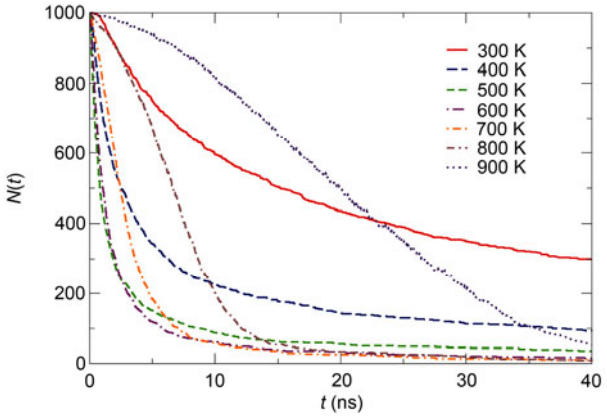

Figure 2 (Color online) Total number of particles $N(t)$ evolves with time at different temperatures with an initial concentration of 0.0133 mol/L (a=50 nm).

900 K becomes faster than those at 700 K and 800 K, be cause the 1000 silver atoms have aggregated into several large clusters. These clusters have limited diffusion, because of their large masses, and the attraction between them again dominates at higher temperatures.

Since the aggregation is almost irreversible, we may consider each aggregation event as an elementary reaction, forming metallic bonds between silver atoms. If all the aggregating particles are of the same size and the system has a constant volume, the time dependence of $N(t)$ can be roughly expressed through the reaction rate of a first-order elementary reaction [29],

$$\frac{\mathrm{d}N(t)}{\mathrm{d}t} = -KN(t). \tag{5}$$

Here, K is the elementary reaction rate constant, and $N(0)$ is the initial total number of individual particles. In a mixture of particles with different sizes, there are many different elementary reactions. For particles with i atoms,

$$\frac{\mathrm{d}N_i(t)}{\mathrm{d}t} = -K_iN_i(t), \tag{6}$$

with K_i the elementary reaction rate constant of particles with i atoms. If the reaction time is relatively short, we can approximately assume that, on average, the elementary reaction of particles with i atoms is independent of the elementary reactions of other particles. Then from eqs. (5) and (6), the time dependent $N(t)$ is the sum of contributions from the time-dependent $N_i(t)$ for all possible values of i,

$$\begin{aligned} &\frac{\mathrm{d}N(t)}{\mathrm{d}t} = -\sum_i K_iN_i(t), \\ &N(t) = \sum_i N_i(0)\exp(-t/\tau_i). \end{aligned} \tag{7}$$

Here, $N_i(0)$, i=1, 2, 3 ... are all constants, and τ_i=1/K_i. For all our MD simulation results, we found that a 3-exponent fitting function form of eq. (7) fits the $N(t)$ curve well. This might imply that the aggregation of the clusters containing one, two, and three atoms forms the major part of the fast process.

In Figure 3, we show the plots of $N(t)$ for the systems with different concentrations at T=300 K. We also show the 3-exponent fitting curve of $N(t)$ at T=300 K with a=25 nm, most of which overlaps with the $N(t)$ curve. The $N(t)$ curves at other concentrations were also fitted by the 3-exponent function, and the coefficients are listed in Table 1. We can see that the decay time is smaller at higher concentrations, which indicates that the reaction time of the elementary reactions decreases at higher concentrations and the whole aggregation process becomes faster. However, it is difficult to use the coefficients of the 3-exponent functions to quantify and analyze the aggregation kinetics. Therefore, we also fit $N(t)$ by the 1-exponent function,

$$N(t) = N(0)\exp(-t/\tau). \tag{8}$$

The 1-exponent fitting curve of $N(t)$ at T=300 K with a=25 nm is also plotted in Figure 3. Despite the noticeable deviation, the fitted curve still somehow follows the decay of $N(t)$. All the $N(t)$ curves at T=300 K were fitted by the 1-exponent function in eq. (8) and the obtained decay times τ are also listed in Table 1. We can see that τ is larger at lower concentrations, consistent with the results plotted in Figure 3.

The decay times τ of the 1000-atom system simulated at different temperatures and concentrations were fitted and are plotted in Figure 4. At the same concentration, τ first decreases with T since the attraction between atoms dominates, and then increases with T since the diffusion dominates and the particles move randomly to explore a higher volume of free space. It can be noted that for all concentrations, τ becomes minimal at around T=600 K. This may indicate that the effects of attraction and diffusion balance at around 600 K, independent of concentration.

The size distributions N_i of the aggregated clusters with size i and an initial concentration of c= 0.0133 mol/L (a= 50 nm) at different temperatures are plotted in Figure 5. We can see that at T= 300 K (Figure 5(a)), the size distributions of the formed clusters at different times are generally quite

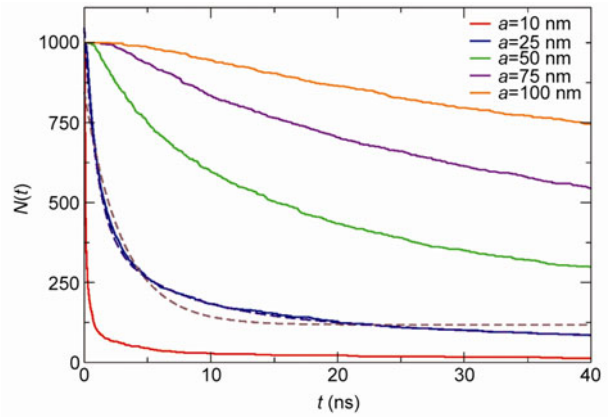

Figure 3 Time dependence of the total number of particles $N(t)$ at different concentrations with different side lengths of simulation cell a at T=300 K. The 3-exponent fitting curve for $N(t)$ with a=25 nm is shown in violet long dashed line and the 1-exponent fitting curve is shown in brown short dashed line.

Table 1 Aggregation decay times, τ_1, τ_2, τ_3, τ, of 3-exponent and 1-exponent fitting functions for $N(t)$ at 300 K, respectively, for the systems with different original side lengths of the periodic cubic simulation box a, and their corresponding concentrations c

a (nm)	c (mol/L)	τ_1 (ns)	τ_2 (ns)	τ_3 (ns)	τ (ns)
10	1.66	0.04360	0.3872	5.284	0.5800
25	0.106	0.9960	5.588	42.58	6.056
50	0.0133	5.128	22.83	22.84	12.47
75	0.00393	1.900	23.84	171.9	41.49
100	0.00166	4.248	80.60	13060.9	102.5

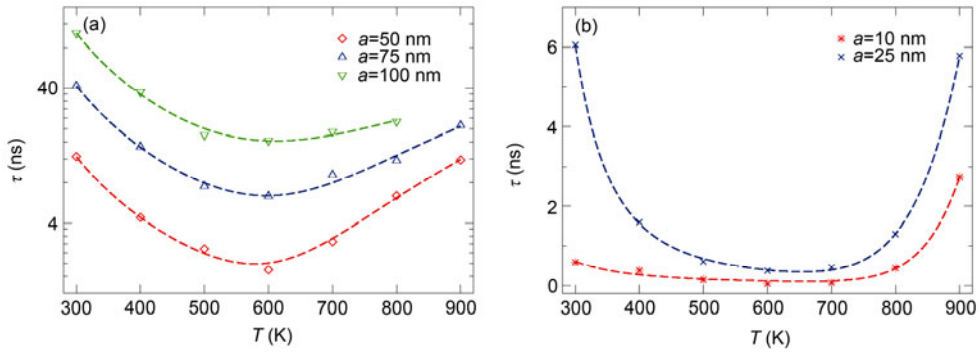

Figure 4 (Color online) Aggregation decay time τ at different concentrations vs. temperature. The symbols are decay times fitted from simulation data and the dashed lines are the fitting of the decay times according to the phenomenological model in eq. (12).

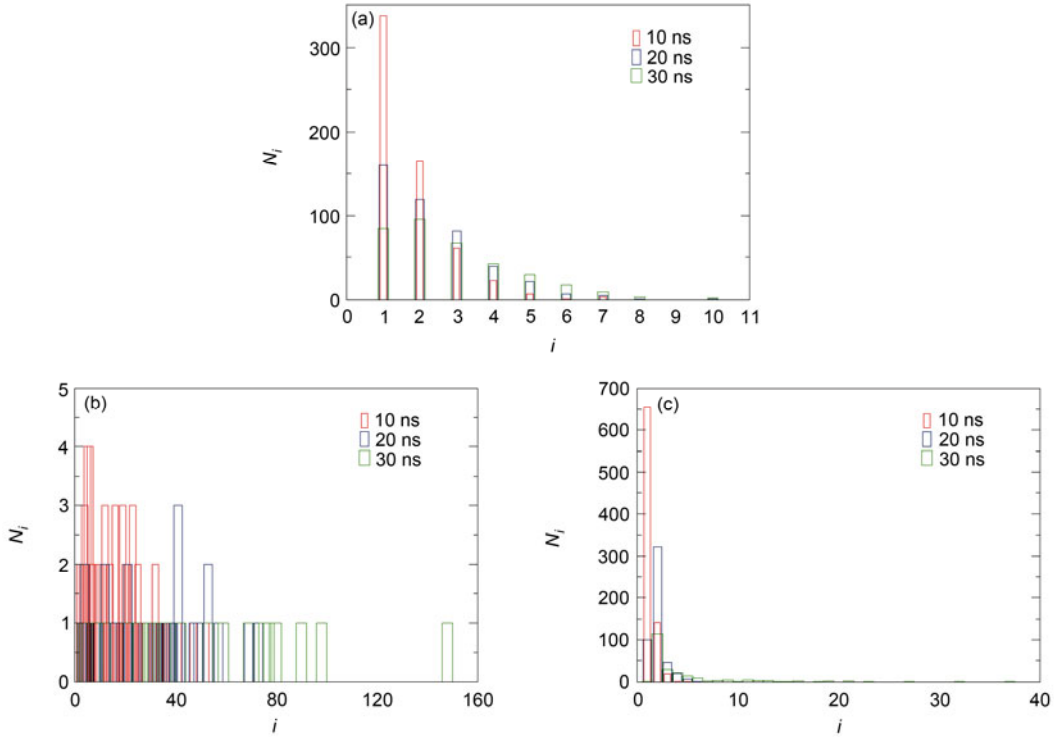

Figure 5 (Color online) Size distribution of aggregated clusters at different times during the aggregation of the system with concentration c= 0.0133 mol/L (a=50 nm) at different temperatures of 300 K (a), 600 K (b), and 900 K (c).

narrow. At t=10 ns, most of the silver atoms have not yet aggregated and only a few silver atoms have aggregated into dimers. Some larger clusters with sizes between 4 to 10 atoms emerge at t= 20 ns and more such clusters emerge at t= 30 ns. At T= 600 K (Figure 5(b)), the size distributions are very wide. At t= 10 ns, the silver atoms aggregate quickly into 61 clusters with their sizes ranging from 1 to 52 atoms. At t=20 ns, these atoms and clusters aggregate into 33 larger clusters ranging from 3 to 73 atoms. At t= 30 ns, the silver clusters further aggregate into 21 large clusters ranging from 3 to 148 atoms and the distribution becomes wider and increasingly discrete. At T= 900 K, at t= 10 ns, the clusters mostly have the sizes between 1 to 5 atoms. The aggregation is slower than that at 600 K, because the diffusion of clusters is dominant at such a high temperature. At t= 20 ns, these silver atoms and clusters aggregate into more silver dimers and some larger clusters contain up to 6 atoms. At t=30 ns, the distribution becomes much wider and the silver clusters have aggregated into larger clusters with sizes between 1 to 37 atoms. In general, the size distribution is wider and considerably more discrete at later stages of aggregation. At T<600 K, the distribution becomes wider at higher temperatures, and at T>600 K, the distribution becomes narrower at higher temperatures.

4 Phenomenological model

In order to help understanding the competition between attraction and diffusion, we then develop a phenomenological model to quantify the temperature dependence of decay time. By means of a mean field approximation, τ can be

understood as the average time for two particles to meet with each other, as illustrated in Figure 6. The transition path sampling theory [30] introduced the concept of transition path ensembles, and demonstrated that the dynamical path probability can be expressed as a product of short-time transition probabilities,

$$P[x(t)] = \rho(x_0)\prod_{i=0}^{L-1} p(x_{i\Delta t} \to x_{(i+1)\Delta t}). \quad (9)$$

Here, $\rho(x_0)$ denotes the distribution of the initial state x_0 of a trajectory $x(t)$. For instance, the distribution may obey the canonical ensemble, $\rho(x_0)\propto\exp[-\beta H(x)]$, where $H(x)$ is the Hamiltonian of the system. $p(x_{i\Delta t}\to x_{(i+1)\Delta t})$ is the transition probability of the process when the state $x_{i\Delta t}$ evolves into the state $x_{(i+1)\Delta t}$. Both $\rho(x_0)$ and $p(x_{i\Delta t}\to x_{(i+1)\Delta t})$ are normalized. In the mean field approximation of our systems, there is also an infinite number of possible reaction paths for two particles to approach and meet, thus τ is the temperature-dependent ensemble average of the reaction time of those paths,

$$\tau(T) = \int P(l,T)\tau(l,T)\delta l, \quad (10)$$

where $P(l, T)$ and $\tau(l, T)$ are the temperature-dependent probability and reaction time of a reaction path l. Because the particle velocities are proportional to $\sqrt{T}$, $\tau(l, T)=C(l)\sqrt{T}$, where $C(l)$ is a function of path l. Similar to the transition path sampling theory [30], we assume the probability of taking a certain reaction path obeys the Boltzmann distribution,

$$\begin{aligned} P(l,T) &= \exp(-E(l)/k_B T)/Z, \\ Z &= \int \exp(-E(l)/k_B T)\delta l, \end{aligned} \quad (11)$$

where $E(l)$ is a collective energy term that might correspond to the Hamiltonian term $H(x)$ in eq. (9). We further cluster the reaction paths into two types: aggregation paths and dissociation paths. The aggregation paths are those along which two particles move towards each other, and the dissociation paths are those along which two particles initially move far away from each other before moving closer. Therefore, the average reaction time can be written as:

$$\begin{aligned} \tau(T) &= \int (P_a(l,T) + P_d(l,T))\tau(l,T)\,\delta l \\ &= \frac{1}{Z\sqrt{T}}\left(\int_a \exp(-E(l_a)/k_B T)C(l_a)\delta l_a \right. \\ &\quad \left. + \int_d \exp(-E(l_d)/k_B T)C(l_d)\delta l_d \right) \\ &\approx \frac{1}{\sqrt{T}}(g_a \exp(-\bar{E}_a/k_B T) + g_d \exp(-\bar{E}_d/k_B T)). \end{aligned} \quad (12)$$

In the above expressions, we made approximations to derive the final equation, where $\bar{E}_a, \bar{E}_d$ are the effective average energies for aggregation and dissociation paths, respectively, and g_a, g_d are constants that reflect the effective weights of aggregation and dissociation paths, respectively. The physical interpretation of the above equation is as the following. Because attraction dominates at low temperatures, particles mainly move along the shorter aggregation reaction paths. At higher temperatures, diffusion dominates and particles have more probabilities to move along the longer dissociation reaction paths. Conversely, particles move faster at higher temperatures. The competition between aggregation and diffusion quantified by eq. (12) results in the change of τ from being smaller to larger with increasing temperatures, as shown in Figure 4. We fitted the temperature dependence of τ at different concentrations by eq. (12), and plot the fitted curves in Figure 4. The fitted values of g_a, g_d, $\bar{E}_a$, and $\bar{E}_d$ are listed in Table 2. The fitting is satisfactory, indicating that our phenomenological model captures the essence of the aggregation and dissociation competition mechanism.

The concentration dependence is included in the fitted constants g_a, g_d, $\bar{E}_a$, and $\bar{E}_d$. From Table 2, we can see that g_a increases and g_d decreases with decreasing concentrations. This may indicate that more particles aggregate by moving towards each other at lower concentrations. However, the development of a quantitative relation between τ and concentration c may be complex and beyond the scope of this work.

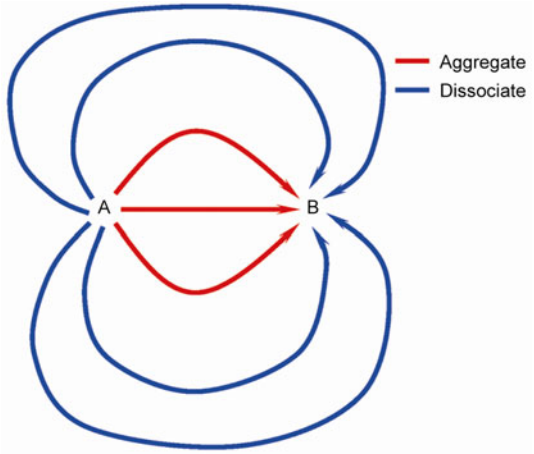

Figure 6 Schematic illustration of the reaction paths of the aggregation process. The red paths are those along which atoms move towards each other, and the blue paths are those along which atoms initially move away from each other and later move towards each other.

Table 2 Fitted values of g_a, g_d, $\bar{E}_a$, and $\bar{E}_d$, with different side lengths of the simulation cell a and the corresponding concentrations c

a (nm)	c (mol/L)	g_a (ns·K$^{1/2}$)	g_d (ns·K$^{1/2}$)	$\bar{E}_a$ (kJ/mol)	$\bar{E}_d$ (kJ/mol)
10	1.66	0.7332	1.326×10^{9}	–6.622	124.3
25	0.106	2.469	5.447×10^{8}	–9.372	112.2
50	0.0133	5.895	2.092×10^{5}	–8.977	48.08
75	0.00393	19.59	1.242×10^{5}	–8.978	40.39
100	0.00166	46.08	3.387×10^{4}	–9.102	28.41

5 Conclusions

The aggregation processes of particles involve two competitive factors: attraction between particles and diffusion of particles. The DLA theory depicts the limited case when interactions between particles are negligible and particle dynamics are only determined by diffusion. In this work, we simulated the non-equilibrium aggregation of silver atoms into silver nanoclusters by MD simulation at different concentrations and temperatures. The aggregation time of silver atoms decreases monotonically with increasing concentration, because at higher concentrations, on average, the particles go through shorter trajectories before they meet and aggregate. With increasing temperature, the aggregation time decreases at T<600 K, then increases at T>600 K. Based on a mean field approximation, a phenomenological model was developed to explain the temperature dependence of the aggregation time as a result of the competition between attraction and diffusion. At T<600 K, self diffusion is weak and attraction dominates, thus particles primarily move towards each other with a higher speed at a higher temperature. At T>600 K, when diffusion dominates, although particles move more rapidly at higher temperatures, they have higher probabilities to move along longer trajectories before they meet and aggregate.

Our simulation results are helpful for understanding the formation mechanism of silver dendrites, particularly the temperature and concentration dependences of the dendritic structure formation. Moreover, this system serves as a model system for understanding the general tendency of non-equilibrium aggregation of nanoscale particles. The conclusions based on the competition between attraction and diffusion should not depend on the details of our simulation model and methods. The developed phenomenological model describing the temperature dependence of the aggregation time may be helpful for understanding the competition between attraction and diffusion in many physical and chemical processes involving aggregation, nucleation, and self-assembly.

This work was supported by the National Natural Science Foundation of China (Grant Nos. 10974208 and 11121403) and the Program of "One Hundred Talented People" of the Chinese Academy of Sciences. Allocations of computer time from the Supercomputing Center in the Computer Network Information Center at the CAS are gratefully acknowledged.

1 Witten T A, Sander L M. Diffusion-limited aggregation, a kinetic critical phenomenon. Phys Rev Lett, 1981, 47: 1400–1403
2 Babu S, Gimel J C, Nicolai T. Diffusion limited cluster aggregation with irreversible slippery bonds. Eur Phys J E, 2008, 27: 297–308
3 Babu S, Gimel J C, Nicolai T, et al. The influence of bond rigidity and cluster diffusion on the self-diffusion of hard spheres with square well interaction. J Chem Phys, 2008, 128: 204504
4 Schmelzer J W P, Röpke G, Priezzhew V B. Nucleation Theory and Applications. Weinheim: Wiley Online Library, 2005
5 McCullagh M, Prytkova T, Tonzani S, et al. Modeling self-assembly processes driven by nonbonded interactions in soft materials. J Phys Chem B, 2008, 112: 10388–10398
6 Wang B, Král P. Optimal atomistic modifications of material surfaces: Design of selective nesting sites for biomolecules. Small, 2007, 3: 580–584
7 Xiu P, Zhou B, Qi W, et al. Manipulating biomolecules with aqueous liquids confined within single-walled nanotubes. J Am Chem Soc, 2009, 131: 2840–2845
8 Kathmann S M, Schenter G K, Garrett B C, et al. Thermodynamics and kinetics of nanoclusters controlling gas-to-particle nucleation. J Phys Chem C, 2009, 113: 10354–10370
9 Wedekind J, Wölk J, Reguera D, et al. Nucleation rate isotherms of argon from molecular dynamics simulations. J Chem Phys, 2007, 127: 154515
10 Ikeshoji T, Hafskjold B, Hashi Y, et al. Molecular dynamics simulation for the formation of magic-number clusters with a Lennard-Jones potential. Phys Rev Lett, 1996, 76: 1792–1795
11 Taboada-Serrano P, Chin C J, Yiacoumi S, et al. Modeling aggregation of colloidal particles. Curr Opin Colloid Interface Sci, 2005, 10: 123–132
12 Pryamtisym V, Ganesan V, Panagiotopoulos A Z, et al. Modeling the anisotropic self-assembly of spherical polymer-grafted nanoparticles. J Chem Phys, 2009, 131: 221102
13 Toxvaerd S. Molecular-dynamics simulation of homogeneous nucleation in the vapor phase. J Chem Phys, 2001, 115: 8913
14 Puertas A M, Odriozola G. Linking phase behavior and reversible colloidal aggregation at low concentrations: Simulations and stochastic mean field theory. J Phys Chem B, 2007, 111: 5564–5572
15 Orrite S D, Stoll S, Schurtenberger P. Off-lattice Monte Carlo simulations of irreversible and reversible aggregation processes. Soft Matter, 2005, 1: 364–371
16 Peters B. Competing nucleation pathways in a mixture of oppositely charged colloids. Out-of-equilibrium nucleation revisited. J Chem Phys, 2009, 131: 244103
17 Thorn M, Broide M L, Seesselberg M. Fluctuations in discrete fragmentation processes studied by stochastic simulations. Phys Rev E, 1995, 51: 4089–4094
18 Odriozola G, Schmitt A, Moncho-Jordá A, et al. Constant bond breakup probability model for reversible aggregation processes. Phys Rev E, 2002, 65: 031405
19 Odriozola G, Schmitt A, Callejas-Fernández J, et al. Simulated reversible aggregation processes for different interparticle potentials: The cluster aging phenomenon. J Phys Chem B, 2003, 107: 2180–2188
20 Smoluchowski M. Drei vortrage uber diffusion, brownsche bewegung und koagulation von kolloidteilchen. Z Phys, 1916, 17: 557–585
21 Smoluchowski M. Versuch einer mathematischen Theorie der Koagulationskinetik kolloider Lösungen. Z Phys Chem, 1917, 92: 129–168
22 Chandrasekhar S. Stochastic problems in physics and astronomy. Rev Mod Phys, 1943, 15: 1–89
23 Plimpton S. Fast parallel algorithms for short-range molecular dynamics. J Comp Phys, 1995, 117: 1–19
24 Daw M S, Baskes M I. Embedded-atom method: Derivation and application to impurities, surfaces, and other defects in metals. Phys Rev B, 1984, 29: 6443–6453
25 Kubo R. The dissipation fluctuation theorem. Rep Prog Phys, 1966, 29: 255–284
26 Freed K F. Long time dynamics of Met-enkephalin: Comparison of explicit and implicit solvent models. Biophy J, 2002, 82: 1791–1808
27 Reynolds O. Papers on mechanical and physical aspects. Phil Trans Soc, 1886, 177: 157
28 Chen Y M, Pearlstein A J. Viscosity-temperature correlation for glycerol-water solutions. Ind Eng Chem Res, 1987, 26: 1670–1672
29 Atkins P W. Concepts in Physical Chemistry. Oxford: Oxford University Press, 2002
30 Dellago C, Bolhuis P G, Geissler P L. Transition path sampling. Adv Chem Phys, 2002, 123: 1–84